JOURNAL OF MATERIALS SCIENCE 31 (1996) 6293–6298

Pore-size determination in the separation layer of a ceramic membrane using the permeation method

P. UCHYTIL
Institute of Chemical Process Fundamentals, Academy of Sciences of the Czech Republic, 165 02 Prague 6, Czech Republic

Results of the determination of the structure parameters of separation layers of ceramic membranes (made of the support and coated by one separation layer) by the gas permeation method are presented. Simultaneously, the difference between the gas flow rate in two orientations (from the separation layer to the support, and vice versa) has been experimentally verified.

1. Introduction

A simple mathematical model describing the gas flow rate, Q, through a ceramic membrane made of a support and one supported (separation) layer, has been proposed [1]. The support and the separation layer have been considered to have a monodisperse porous structure with cylindrical parallel pores. The gas flow rate through each layer has been supposed to be the sum of the Knudsen and Poiseuille flow contributions.

The equations for the evaluation of Knudsen, R_1^k and Poiseuille, R_1^p, flow resistance characteristics of a separation layer by the linear treatment of the experimental permeation data have been suggested [1]. The relation for the ordinary flow orientation, A, the direction from the separation layer to the support, is

$$Q_A P_0/[A(P_1 - P_{2A})] = 1/R_1^k + (P_1 + P_{2A})/(2R_1^p) \quad (1)$$

As has been shown [1], there exists a difference between the values of gas flow rates through the supported membrane from the opposite sides. For the second flow orientation, B, the equation has the form

$$Q_B P_0/[A(P_{2B} - P_3)] = 1/R_1^k + (P_{2B} + P_3)/(2R_1^p) \quad (2)$$

where A is the membrane area, P_0 is the pressure at which the gas flow rate Q is measured (usually the atmospheric one), P_1 and P_3 are pressures at the opposite sides of the membrane and P_2 (P_{2A} for direction A, P_{2B} for direction B) is the pressure at the plane of the contact of the support and the separation layer. The flow resistance characteristics are defined by

$$R_x^p = 8 l_x q_x \eta/(r_x^2 \varepsilon_x) \quad (3)$$

$$R_x^k = 3 l_x q_x [\pi M/(8RT)]^{1/2}/(2 r_x \varepsilon_x) \quad x = l, s \quad (4)$$

where $x = s$ indicates the support properties and $x = l$ the properties of the separation layer, l is the layer thickness, q is the tortuosity of the pore (pore length $l_r = ql$), r is the pore radius, ε is the porosity of the layer, R is the gas constant, T is the absolute temperature, η is the gas viscosity, and M is the molecular weight of the gas used for the permeation measurement.

The pressures P_{2A} and P_{2B} can be calculated from quadratic equations [1] as a function of the gas flow rate, corresponding pressure conditions and from values of the resistance characteristics of the support only (which are determined from the individual permeation measurements of the support)

$$P_{2A} = -R_s^{pk} + [(R_s^{pk})^2 + P_3^2 + 2P_3 R_s^{pk} + 2Q_A P_0 R_s^p/A]^{1/2} \quad (5)$$

$$P_{2B} = -R_s^{pk} + [(R_s^{pk})^2 + P_1^2 + 2P_1 R_s^{pk} - 2Q_B P_0 R_s^p/A]^{1/2} \quad (6)$$

where $R_s^{pk} = R_s^p/R_s^k$.

It is evident from Equations 1 and 2 that the Poiseuille and the Knudsen flow resistance characteristics, R_l^p and R_l^k of a separation layer can be evaluated from the experimental gas permeation data for different conditions of pressures and flow orientations, by the linear regression method. The values of independent parameters $r_l\varepsilon_l/(q_l l_l)$ and $r_l^2\varepsilon_l/(q_l l_l)$ can be evaluated from the Poiseuille and the Knudsen flow resistance characteristics, R_l^p and R_l^k. If several gases are used for the permeation measurements, more reliable values of the parameters $r_l\varepsilon_l/(q_l l_l)$ and $r_l^2\varepsilon_l/(q_l l_l)$ can be obtained from the linear treatment of all gas permeation data together – the dependence $Q_{iA}P_0 M_i^{1/2}/[A(P_1 - P_{2A})]$ on $(P_1 + P_{2A})\, M_i^{1/2}/(2\eta_i)$ for direction A; the dependence for direction B has similar form. Index i refers to the used gas. The analogous relations can be used for the determination of structure parameters of the support, $r_s\varepsilon_s/q_s$ and $r_s^2\varepsilon_s/q_s$. The values of parameters $r_l\varepsilon_l/(q_l l_l)$ and $r_l^2\varepsilon_l/(q_l l_l)$ from the linear treatment

0022–2461

of the gas permeation data can be used as initial values for the non-linear optimization procedure.

The value of the mean pore radius r_l is calculated from the relation

$$r_l = [r_l^2\varepsilon_l)/(q_l l_l)]/[r_l\varepsilon_l/(q_l l_l)] \quad (7)$$

If the separation layer thickness, l, is known, for example from electron microscopy, the value of the geometric factor $\Psi_l = \varepsilon_l/q_l$ can be determined.

Not all types of membranes are suitable for the determination of the structure parameters of the separation layer by the permeation method. In general, ceramic membranes made of a support and one separation layer can be grouped into three main classes.

Class 1. The overall resistance to the gas flow in the supported layer is much higher than in the support. This is the case in a thick ultrafiltration layer with very small pores deposited on a very porous support with large pores. In this case the effect of the support can be neglected.

Class 2. The overall resistance to the gas flow in the supported layer is much lower than in the support. This is the case of a very thin microfiltration layer deposited on a thick support of a comparable pore size. In this case the structure parameters of the supported layer cannot be obtained by the gas permeation method.

Class 3. The overall resistance to the gas flow in both layers is comparable. This case is rather frequent in practice and the suitability of the gas permeation method for the determination of the porous structure of separation layers of ceramic membranes depends on the accuracy of the permeation data. The proposed procedure can give reasonable results for ceramic membranes where the Poiseuille and the Knudsen flow resistances in a separation layer play important roles in the whole resistance of a membrane.

2. Experimental procedure

Two samples of membranes with a comparable gas flow resistance in a separation layer and in a support were selected for the verification of the suitability of the gas permeation method for the determination of the porous structure of the separation layer. Sample 1 was made of α-alumina (support and separation layer, Gerasiv GmbH, Germany); the support of sample 2 was made of carbon and the separation layer of zirconium oxide.

All the permeation measurements were carried out in a stainless steel cell at the same temperature, 293 K, and the gas flow rate was measured at atmospheric pressure $P_0 = 0.1$ MPa.

For the characterization of the porous structure of supports, the following methods and devices were used.

1. Mercury porosimetry (mercury porosimeter AutoPore 9200, Micromeritics, USA).
2. Permeation method (laboratory apparatus).
3. Helium pycnometer (AutoPycnometer 1320, Micromeritics, USA).

3. Results and discussion

3.1. Characterization of the porous structure of the support

The linear dependencies of the permeability of gas i, $Q_iP_0/[A(P_1 - P_3)]$ on the arithmetic mean gas pressure, $\bar{P}$, in supports of samples 1 and 2 can be seen in Figs 1 and 2. Hydrogen, nitrogen and carbon dioxide were employed for the permeation measurements of sample 1; in the case of sample 2, oxygen, helium and methane were also used.

The values of the structure parameters r_s and ε_s of the supports obtained from the permeation experiments, mercury porosimetry and helium pycnometer, are presented in Table I. The linear treatment of all permeation data together was used, see Figs 3 and 4.

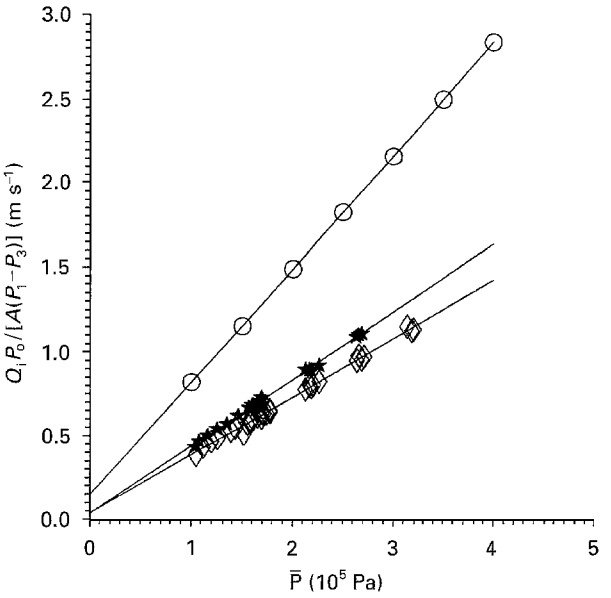

Figure 1. Dependence of the gas permeability, $Q_iP_0/[A(P_1 - P_3)]$ on the arithmetic mean gas pressure, $\bar{P}$, in the support of sample 1. (○) H_2, (◇) N_2, (★) CO_2.

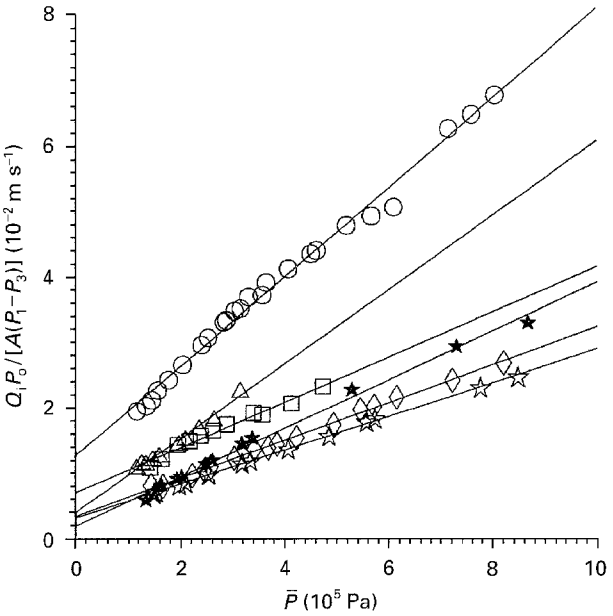

Figure 2. Dependence of the gas permeability, $Q_iP_0/[A(P_1 - P_3)]$ on the arithmetic mean gas pressure, $\bar{P}$, in the support of sample 2. (○) H_2, (◇) N_2, (★) CO_2, (△) CH_4, (□) He, (☆) O_2.

TABLE I Thickness, mean pore radius, porosity and geometric factor of the support. Hg indicates results of mercury porosimetry, and per indicates the permeation method. Values of porosity, ε_{He}, were calculated from the results of helium pycnometry (the value of bulk density was used from mercury porosimetry)

Support	l (mm)	r_{Hg} (μm)	r_{per} (μm)	ε_{He}	ε_{per}	Ψ_{per}
Sample 1	1.8	3.0	3.0	0.29	0.28	0.081
Sample 2	2.0	0.1	0.35	0.31	0.26	0.070

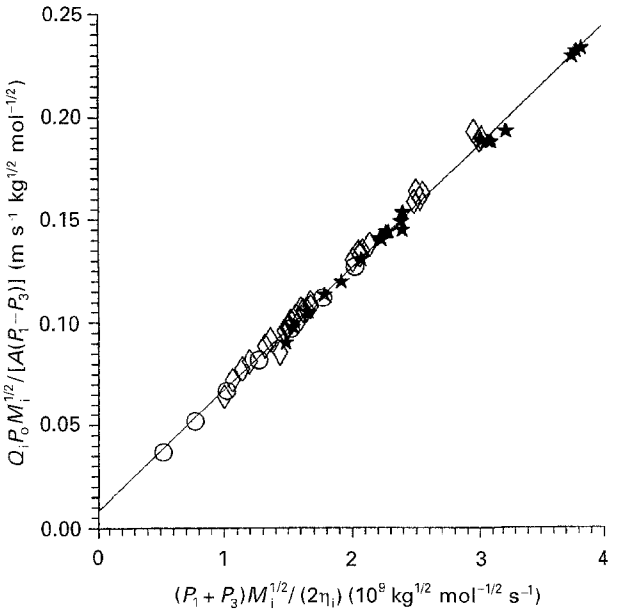

Figure 3. Determination of parameters $r_s\varepsilon_s/q_s$ and $r_s^2\varepsilon_s/q_s$ of sample 1 from linear treatment of the dependence of gas permeation data $Q_iP_0M_i^{1/2}/[A(P_1 - P_3)]$ on $(P_1 + P_3)\ M_i^{1/2}/(2\eta_i)$. (○) H_2, (◇) N_2, (★) CO_2.

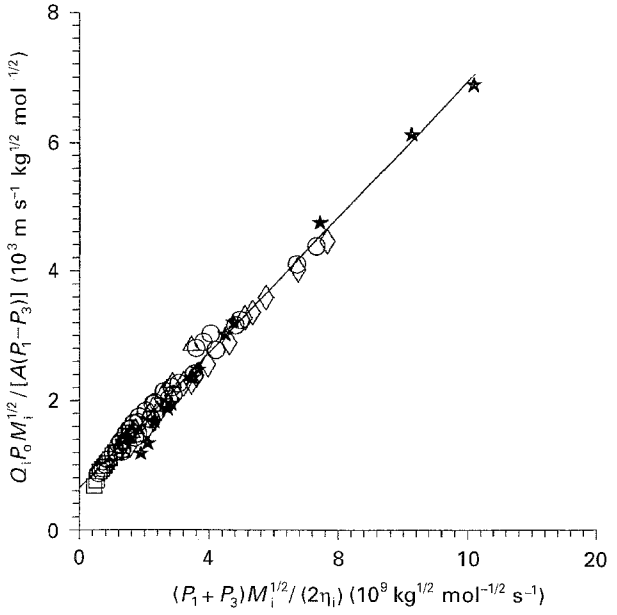

Figure 4. Determination of parameters $r_s\varepsilon_s/q_s$ and $r_s^2\varepsilon_s/q_s$ of sample 2 from linear treatment of the dependence of the gas permeation data $Q_iP_0M_i^{1/2}/[A(P_1 - P_3)]$ on $(P_1 + P_3)\ M_i^{1/2}/(2\eta_i)$. (○) H_2, (◇) N_2 (★) CO_2, (△) CH_4, (□) He, (☆) O_2.

Good agreement between the results of the permeation measurements and the mercury porosimetry can be seen.

The pore-size distribution from the mercury porosimetry of sample 1 is plotted in Fig. 5, and the distribution of sample 2 in Fig. 6. Better agreement between the pore size determined by mercury porosimetry (the pore radius corresponds to the maximum differential distribution of the pore volume) and the permeation method can be expected for the samples with narrow pore-size distribution (sample 1). In the case of the polydisperse character (sample 2) of a material, the agreement will be inferior. In addition, greater values of porosity determined by the combination of the results of helium pycnometry and mercury porosimetry than from the permeation measurements, are not surprising. This fact is caused by differences

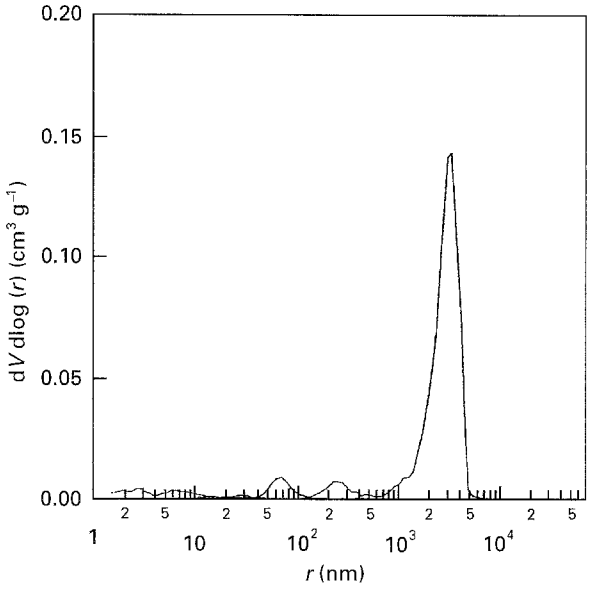

Figure 5. Pore-size distribution of the support of sample 1 from mercury porosimetry.

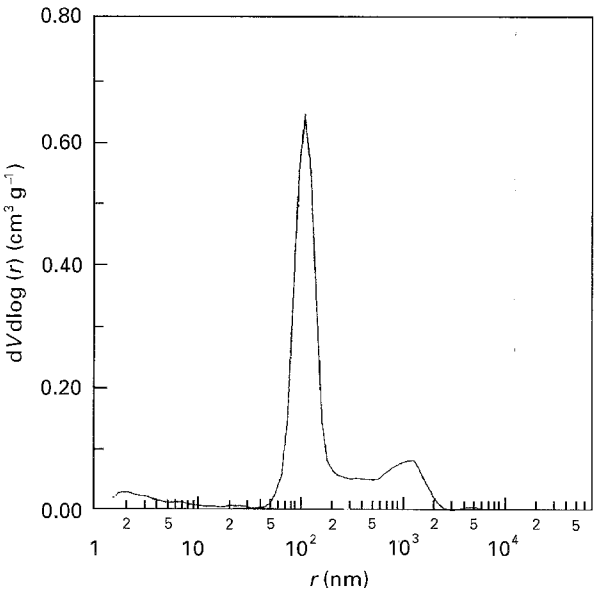

Figure 6. Pore-size distribution of the support of sample 2 from mercury porosimetry.

in the physical principle of both methods; the permeation method evaluates only the porosity of transport pores, whereas the results of the second method also include the contribution of blind pores.

3.2. Characterization of the porous structure of the separation layer

Fig. 7 shows the dependence of hydrogen permeability $Q_iP_0/[A(P_1 - P_3)]$ for the same support as sample 1 (line 1), and the same support with a separation layer (line 2), on the arithmetic mean gas pressure in the membrane, $\bar{P}$. Pressure drop, ΔP, in the membrane is $\Delta P = P_1 - P_3$, where pressure P_3 at the membrane outlet is atmospheric pressure, $P_3 = 0.1$ MPa. In Fig. 7, a great difference between hydrogen flow rates through the support and the complete membrane can be seen. The Poiseuille flow contribution to the overall gas flow rate is evident from the slopes of lines 1 and 2. The flow resistance in the separation layer is high and the value of the Poiseuille flow contribution to the overall flow cannot be neglected. Similar results were obtained for sample 2. It is concluded that these membranes are appropriate for the determination of the structure parameters of the separation layer by the permeation method.

The hydrogen permeability for two gas flow orientations, A and B, in sample 1 is compared in Fig. 8. For each value of pressure, P_3, at the membrane outlet ($P_3 = 0.1$, 0.2 and 0.3 MPa) two branches of hydrogen permeability dependence, $Q_iP_0/[A(P_1 - P_3)]$ on the arithmetic mean gas pressure $\bar{P}$ in the membrane, are seen. Branch A corresponds to the ordinary flow orientation in the direction from the supported layer to the support. It follows from Fig. 8, that the gas permeabilities are higher for direction B, which is in agreement with the results obtained from the mathematical modelling [1]. This fact leads to a more precise evaluation of the flow resistance characteristics of the separation layer when the permeation data obtained for gas flow orientation A was selected for the permeation measurements. Branches A and B start from the same values of the ordinate $Q_iP_0/[A(P_1 - P_3)]$ at the value of pressure, $\bar{P}$, which corresponds to the trivial case of the zero pressure drop across the membrane, $\Delta P = 0$ ($P_1 = P_3 = P_2 = \bar{P}$), and zero gas flow rate across the membrane.

The treatment of the permeation data of sample 1 for individual gases (H_2, N_2 and CO_2) according to Equation 1 was made to compare the gas flow resistance in the support and in the separation layer. The values of the Poiseuille and the Knudsen flow resistance characteristics of the support and of the separation layer (sample 1) are given in Table II.

From the comparison of the results of permeation measurements mentioned in Table II, it is evident that the resistance to gas flow is higher in the separation layer – especially the Poiseuille term. The Poiseuille flow contribution is predominant in the support. This fact is in accordance with the physical sense – the importance of the Poiseuille flow contribution increases with increasing pore size (the pore size in the support is greater than in the separation layer). In the case of the separation layer, the values the Knudsen

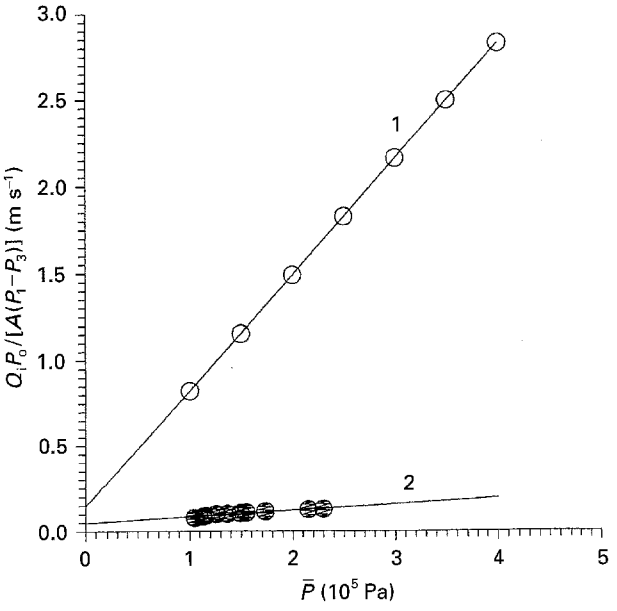

Figure 7. Dependence of hydrogen permeability $Q_iP_0/[A(P_1 - P_3)]$ on the arithmetic mean gas pressure, $\bar{P}$, in support 1 and the support with separation layer 2; sample 1. Outlet pressure $P_3 = 0.1$ MPa, gas flow orientation from separation layer to support A.

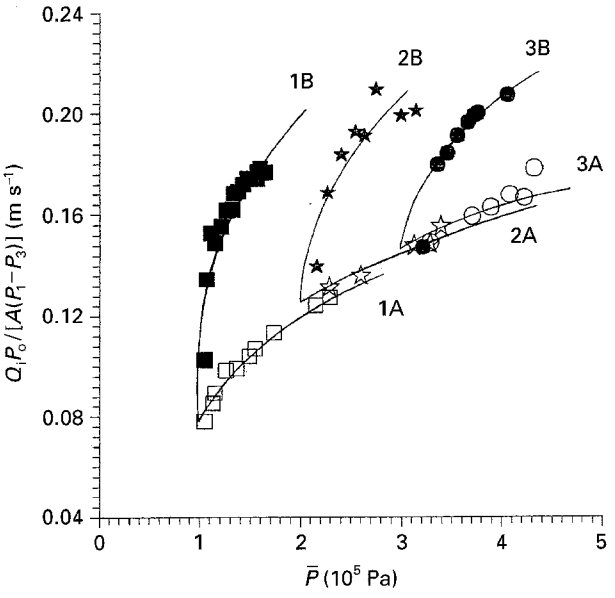

Figure 8. Dependence of hydrogen permeability $Q_iP_0/[A(P_1 - P_3)]$ on the arithmetic mean gas pressure, $\bar{P}$, in sample 1 for both directions A and B, for different values of outlet pressure $P_3 = 0.1$ MPa (line 1), 0.2 MPa (line 2), 0.3 MPa (line 3).

TABLE II The values of the Poiseuille and Knudsen flow resistance characteristics of the support and the separation layer of sample 1 evaluated from the individual gas permeation data

Gas	R^k_{si} (s m^{-1})	R^p_{si} (10^5 Pa s m^{-1})	R^k_{li} (s m^{-1})	R^p_{li} (10^5 Pa s m^{-1})
Hydrogen	6.80	1.49	12.4	41.9
Nitrogen	23.2	2.90	36.4	75.8
Carbon dioxide	29.5	2.49	34.7	76.0

and the Poiseuille flow contributions under our experimental conditions, are comparable (see Equation 1, the reciprocal value of the Poiseuille flow resistance characteristic must be multiplied by the arithmetic mean gas pressure, $\bar{P}$, in the layer).

The values of the structure parameters of the separation layers of samples 1 and 2 calculated from the linear treatment of all permeation data together (the dependence $Q_{iA}P_0M_i^{1/2}/[A(P_1 - P_{2A})]$ on $(P_1 + P_{2A})$ $M_i^{1/2}/(2\eta_i)$) can be seen in Table III and in Figs 9 and 10. Hydrogen, nitrogen and carbon dioxide were used for the permeation measurements of sample 1; in the case of sample 2, oxygen and helium were also used. The hydrogen permeation data were not used for the evaluation of the structure parameters of the separation layer of sample 2. Hydrogen permeability was significantly greater in comparison with other gases; this fact can be explained by the so-called "surface diffusion" of hydrogen on the surface of zirconium oxide. For example, Yamaki *et al.* [2] observed the increase of the permselectivity of hydrogen to nitrogen with repetition of the impregnation cycle of a γ-alumina porous membrane by zirconium oxide particles.

The value of the separation layer thickness of the membranes was obtained from electron micrographs, see Figs 11 and 12. The values of porosity, ε_1, were estimated from the geometric factor $\Psi_1 = \varepsilon_1/q_1$, assuming that $q_1 = 1/\varepsilon_1$.

Initially, it was intended to use a non-linear optimization method for the determination of the structure parameters of the separation layers with initial values obtained from the linear treatment of the permeation data. However, in reality, the application of a non-linear optimization method was not advantageous. This method is numerically unstable and the obtained minimum is flat. Therefore, the structure parameters can be estimated only with difficulty and are computation time-demanding. The results calculated from the linear dependence are not significantly different.

The bubble point method was used for the characterization of the quality of the separation layer for the qualitative indication of the largest pores (defects) in

TABLE III The values of the structure parameters of the separation layer of samples 1 and 2 evaluated from the permeation data

Sample	l_1 (μm)	r_1 (μm)	$\Psi_1 = \varepsilon_1/q_1$	ε_1
1	60	0.238	0.018	0.13
2	10	0.095	0.0030	0.055

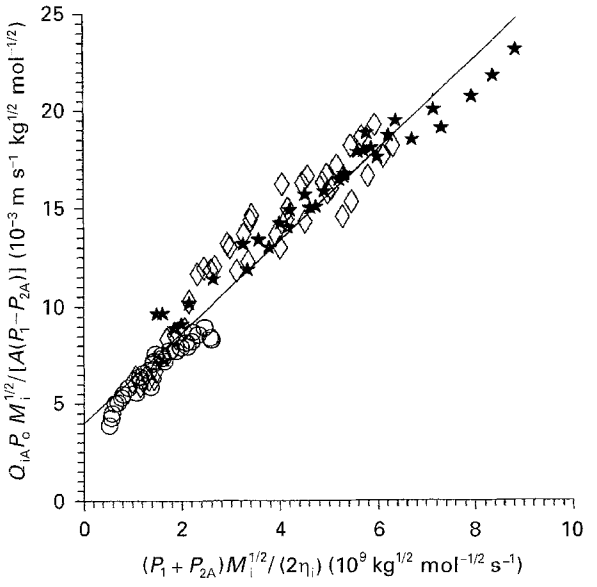

Figure 9. Determination of parameters $r_1\varepsilon_1/(q_1l_1)$ and $r_1^2\varepsilon_1/q_1l_1)$ of sample 1 from linear treatment of the dependence of all gas permeation data $Q_{iA}P_0M_i^{1/2}/[A(P_1 - P_{2A})]$ on $(P_1 + P_{2A})$ $M_i^{1/2}/(2\eta_i)$. (○) H_2, (◇) N_2, (★) CO_2.

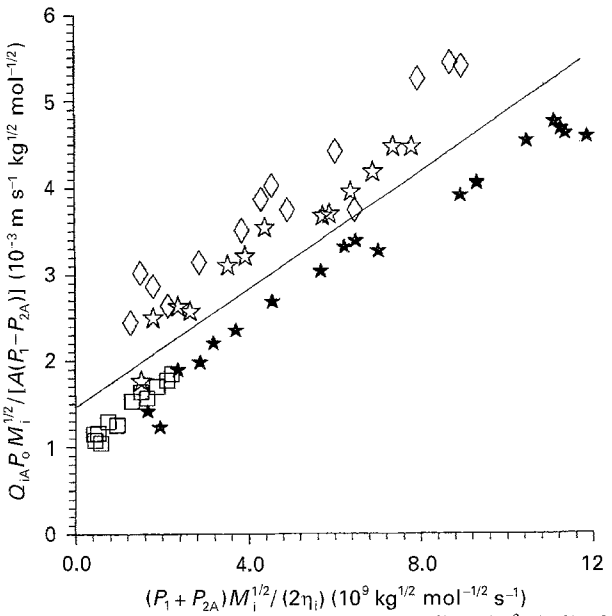

Figure 10. Determination of parameters $r_1\varepsilon_1/(q_1l_1)$ and $r_1^2\varepsilon_1/(q_1l_1)$ of sample 2 from linear treatment of the dependence of all gas permeation data $Q_{iA}P_0M_i^{1/2}/[A(P_1 - P_{2A})]$ on $(P_1 + P_{2A})$ $M_i^{1/2}/(2\eta_i)$. (◇) N_2, (★) CO_2, (□) He, (☆) O_2.

Figure 11. Scanning electron micrograph of the support and separation layer of sample 1.

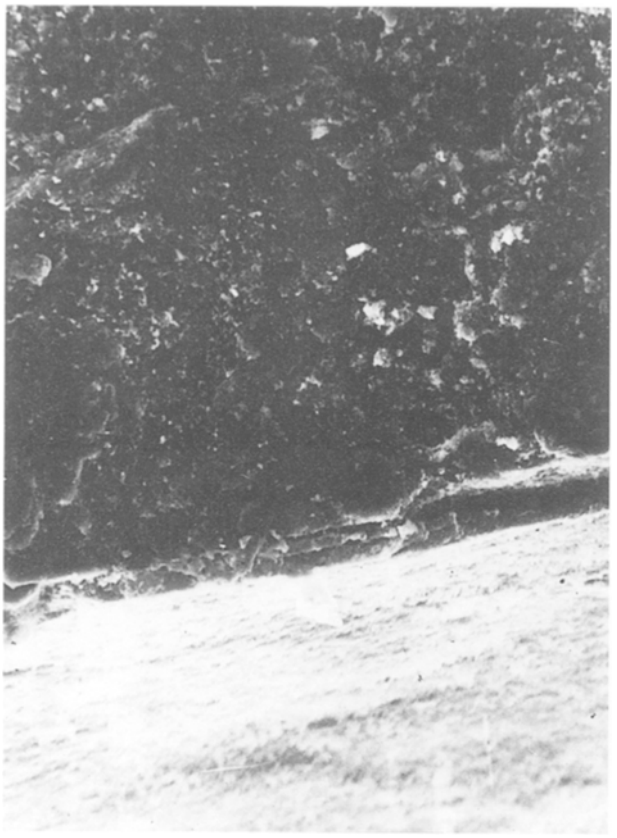

Figure 12. Scanning electron micrograph of the support and separation layer of sample 2.

TABLE IV Results of the bubble point test of samples 1 and 2

Sample	ΔP (10^5 Pa)	Number of pores	r (μm)
1	1.66	1	0.88
	1.74	3	0.84
	2.05	4	0.71
	2.30	10	0.63
2	0.62	1	2.35
	0.64	3	2.28
	0.65	5	2.24
	0.66	10	2.21

the separation layer, see Table IV. Before measurement, the samples were filled with distilled water under vacuum and then the gas pressure on one side of the membrane was increased; the pressure on the opposite side was atmospheric. Water was expelled from the pores of radius r at a pressure difference, ΔP, according to the Washburn equation

$$r = 2\gamma \cos\phi/\Delta P \tag{8}$$

The values used for the calculation of pore radii were $\gamma = 72.8 \times 10^{-3}$ N m^{-1} and $\cos\phi = 1$. The number of pores given in Table IV is the number of pores with pore radius greater or equal to the value of r.

From a comparison of the values of the mean pore radius of the support and of the separation layer obtained from permeation measurements, with the estimated values of the greatest pores in the separation layer obtained by the bubble point method for both samples (see Table V), it is evident that in the supports there are some places which are not fully covered by the separation layer (the size of the defects responds approximately to the size of the pores in the supports).

TABLE V Comparison of the size of membrane defects estimated by the bubble point method with the values of pore radii in the separation layer and the support for both samples, determined by the permeation method

Sample	r_s (μm)	r_1 (μm)	r_b (μm)
1	3.0	0.238	2.35
2	0.35	0.095	0.88

4. Conclusion

A new linearization procedure for the treatment of the gas permeation data was used for the determination of the mean pore size of the pores in the separation layer and for the estimation of its porosity. The application of the proposed method is limited by the accuracy of the permeation measurements and by the relation between the values of the flow resistances of the support and the separation layer.

It was experimentally demonstrated that the permeabilities depend not only on pressures P_1 and P_3 but also on the selected gas flow orientation through the membrane. Two branches of the dependence of permeability on the arithmetic mean gas pressure, $\bar{P}$, in the membrane exist, one for the ordinary flow orientation in the direction from the separation layer to the support (A) and the other for the opposite direction (B). Higher gas flow rates correspond to direction B.

Direction A of the gas flow is more advantageous for the evaluation of the structure parameters of the separation layer, because the gas flow resistance in this direction is greater and the resistance characteristics thus can be determined with higher accuracy.

In conclusion, the gas permeation method is not suitable for the determination of the structure characteristics of the separation layers with a small gas flow resistance. The characterization of separation layers with very small pore sizes ($r < 10$ nm) is also impossible, because there is a negligible contribution of the Poiseuille flow term.

Acknowledgment

Valuable discussions with Dr J. Roček are gratefully acknowledged.

References

1. P. UCHYTIL and Z. BROŽ, *J. Membrane Sci.* **97** (1994) 145.
2. T. YAMAKI, H. MAEDA, K. KUSAKABE and S. MOROOKA, *ibid.* **85** (1993) 167.

Received 20 April 1995
and accepted 8 May 1996